Discrete geometry for reliable surface quad-remeshing

Konrad Polthier and Faniry Razafindrazaka

Abstract In this overview paper we will glimpse how new concepts from discrete differential geometry help to provide a unifying vertical path through parts of the geometry processing pipeline towards a more reliable interaction. As an example, we will introduce some concepts from discrete differential geometry and the QuadCover algorithm for quadrilateral surface parametrization. QuadCover uses exact discrete differential geometric concepts to convert a pair (simplicial surface, guiding frame field) to a global quad-parametrization of the unstructured surface mesh. Reliability and robustness is an omnipresent issue in geometry processing and computer aided geometric design since its beginning. For example, the variety of incompatible data structures for geometric shapes severely limits a reliable exchange of geometric shapes among different CAD systems as well as a unifying mathematical theory. Here the integrable nature of the discrete differential geometric theory and its presented application to an effective remeshing algorithm may serve an example to envision an increased reliability along the geometry processing pipeline through a consistent processing theory.

1 Calculus on Simplicial Surfaces

We begin with a 2-dimensional simplicial surface $M_h \subset \mathbb{R}^n$ where n is typically in $\{2, 3, 4\}$. On a simplicial surface M_h we consider two types of piecewise linear (PL) function spaces, the *conforming Lagrange space* $S_h(M_h)$ and the *non-conforming space* $S_h^*(M_h)$. Both spaces are classic in finite element literature, but here we will see how both function spaces team up to mimic

Konrad Polthier
Freie Universität Berlin, e-mail: konrad.polthier@fu-berlin.de

Faniry Razafindrazaka
Freie Universität Berlin, e-mail: faniry.razafi@fu-berlin.de

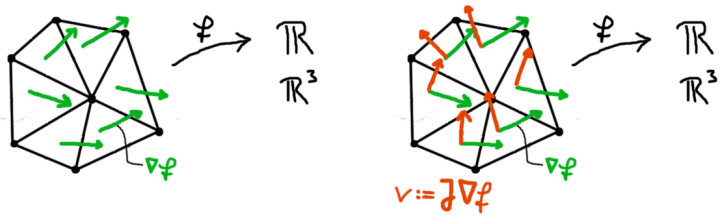

Fig. 1 Gradient field ∇f and co-gradient field $\delta f := J\nabla f$ are constant on each triangle.

the concept of primality and duality of grids in the framework of function spaces on the *same* underlying geometry, thus allowing to use the simplicial surface M_h as single base geometry. For example, solutions of the discrete Cauchy-Riemann equations will consist of a pair of a discrete conforming and non-conforming harmonic map in S_h and in S_h^* resp. vice versa, all defined on M_h .

Definition 1. The *piecewise linear conforming* $S_h(M_h)$ *and non-conforming* $S_h^*(M_h)$ *function spaces* on a 2-dimensional simplicial surface $M_h \subset \mathbb{R}^n$ are given by:

$$S_h := \left\{ f : M_h \to \mathbb{R} \;\middle|\; f_{|T} \text{ is linear on each triangle } T, \text{ and } f \in C^0\left(M_h\right) \right\}$$
$$S_h^* := \left\{ f^* : M_h \to \mathbb{R} \;\middle|\; f_{|T}^* \text{ is linear, and continuous at edge midpoints} \right\}$$

On first sight, the missing global continuity of functions $f^* \in S_h^*$ sounds like a drawback but the space of non-conforming functions will turn out as a good match to S_h, see Figure 3 for the graphs of two sample functions. Both function types have gradients from piecewise differentiation:

Definition 2. The *gradient field* ∇f of a function $f \in S_h$ or S_h^* is a constant tangent vector in each triangle. The *co-gradient field* $\delta f := J\nabla f$ is obtained by rotation J of the gradient ∇f, i.e. by $\frac{\pi}{2}$ in each triangle.

1.1 Discrete Vector Fields

Piecewise constant vector fields were introduced to geometry processing in [13] as a natural discretization of tangential vector fields on simplicial geometries. Among the useful properties of PC vector fields, say compared to Whitney type differential forms, are the formulation of the Hodge star operation in function spaces instead of introducing a pair of primary and dual meshes. After a short overview of PC vector fields and their integrability conditions

we touch two sample problems, the discrete Cauchy-Riemann equation and the discrete Hodge decomposition , to highlight the efficiency of PC vector fields and to prepare some tools for the QuadCover application.

Definition 3. The space of *piecewise constant tangential vector fields* $\Lambda^1(M_h)$ on a 2-dimensional simplicial surface $M_h \subset \mathbb{R}^n$ is given by:

$$\Lambda^1(M_h) := \left\{ v : M_h \to TM_h \;\middle|\; v_{|\text{triangle } T} \text{ is a constant tangent vector in } T \right\}$$

The gradient and co-gradients fields of functions in S_h or S_h^* introduced above are examples of piecewise constant (PC) tangential vector fields, see Figure 1

Definition 4. On a simplicial surface M_h let $v \in \Lambda^1(M_h)$, p a vertex and m an edge midpoint. Then the (total) *discrete curl* is given by

$$\operatorname{curl}_h v(p) := \frac{1}{2} \oint_{\partial \operatorname{star} p} v = \frac{1}{2} \sum_{i=1}^{k} \langle v, c_i \rangle$$

$$\operatorname{curl}_h^* v(m) := \oint_{\partial \operatorname{star} m} v = -\left\langle v_{|T_1}, c \right\rangle + \left\langle v_{|T_2}, c \right\rangle$$

where c_i are the edges of the oriented boundary of star p resp. c the edge with midpoint m.

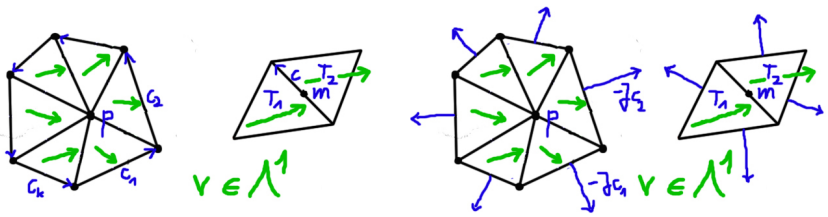

Fig. 2 Discrete curl and divergence operators.

Theorem 1 (Local integrability conditions). *Let M_h be a simply connected simplicial surface . Then a PC vector field $v \in \Lambda^1(M_h)$ can be characterized as gradient field in term of the discrete* curl *operator:*

1. v is a gradient field of a function in S_h $\iff$

$$\operatorname{curl}_h^* v(m) = 0 \text{ at all edge midpoints } m.$$

2. v is a gradient field of a function in S_h^* $\iff$

$$\operatorname{curl}_h v(p) = 0 \text{ at all vertices } p.$$

Definition 5. On a simplicial surface M_h let $v \in \Lambda^1(M_h)$, p a vertex and m an edge midpoint. Then the (total) *discrete divergence* is given by

$$\operatorname{div}_h v(p) := \frac{1}{2} \oint_{\partial \operatorname{star} p} \langle v, \nu \rangle \, ds = -\frac{1}{2} \sum_{i=1}^{k} \langle v, Jc_i \rangle$$

$$\operatorname{div}_h^* v(m) := \oint_{\partial \operatorname{star} m} \langle v, \nu \rangle \, ds = \left\langle v_{|T_1}, J_{|T_1} c \right\rangle + \left\langle v_{|T_2}, J_{|T_2} c \right\rangle$$

where ν is the outer unit normal along $\partial \operatorname{star} p$ resp. $\partial \operatorname{star} m$.

Remark 1. Discrete rotation and divergence are related by $\operatorname{curl}_h Jv = \operatorname{div}_h v$ and $\operatorname{curl}_h^* Jv = \operatorname{div}_h^* v$, compare Figure 2.

1.2 Discrete Cauchy-Riemann Equation

With the first order operators ∇, curl and div at hand we deduce the discrete Laplace-Beltrami operators and a notion of conjugacy of harmonic vector fields.

Definition 6. The *discrete Laplace-Beltrami operator* Δ of functions in S_h resp. in S_h^* on a simplicial surface M_h is given as divergence of the corresponding gradient functions, i.e. $\Delta_h f(p) := \operatorname{div}_h \nabla f(p)$ for $f \in S_h$ and $\Delta_h^* f^*(m) := \operatorname{div}_h^* \nabla f^*(m)$ for $f^* \in S_h^*$.

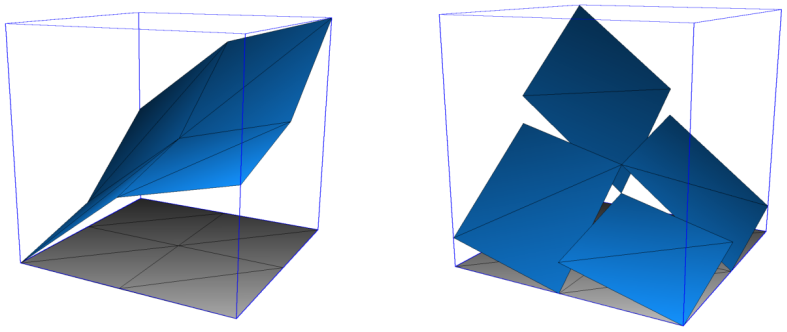

Fig. 3 Graph of a conforming harmonic function $f \in S_h$ and a non-conforming harmonic function $g \in S_h^*$, here satisfying the Cauchy-Riemann equation $\nabla g = \delta f$.

A natural question is the existence of solutions to the discrete Cauchy-Riemann equation which asks for pairs (f, g) of discrete maps f and g with $\nabla g = \delta f$, and thus for discrete holomorphic resp. conformal maps $z = f + ig$.

In the smooth setting, a co-gradient field δf has a potential function g with $\nabla g = \delta f$ if and only if f and g are a pair of conjugate harmonic maps, i.e. real and imaginary parts of a holomorphic map. The discrete Cauchy-Riemann equation holds for a matching pair of a conforming and a non-conforming harmonic function:

Theorem 2 (Cauchy-Riemann equation). *On a simply connected simplicial surface $M_h \subset \mathbb{R}^n$ the harmonic maps in S_h and S_h^* come in conjugate harmonic pairs solving the* discrete Cauchy-Riemann equation $\nabla g = \delta f$ *[12]:*

1. *The co-gradient δf of $f \in S_h$ is a gradient field of a function $g^* \in S_h^*$ $\iff$ f is discrete harmonic in S_h.*
   Furthermore, the conjugate map $g^* \in S_h^*$ is discrete harmonic.
2. *The co-gradient δf^* of $f^* \in S_h^*$ is a gradient field of a function $g \in S_h$ $\iff$ f^* is discrete harmonic in S_h^*.*
   Furthermore, the conjugate map $g \in S_h$ is discrete harmonic.

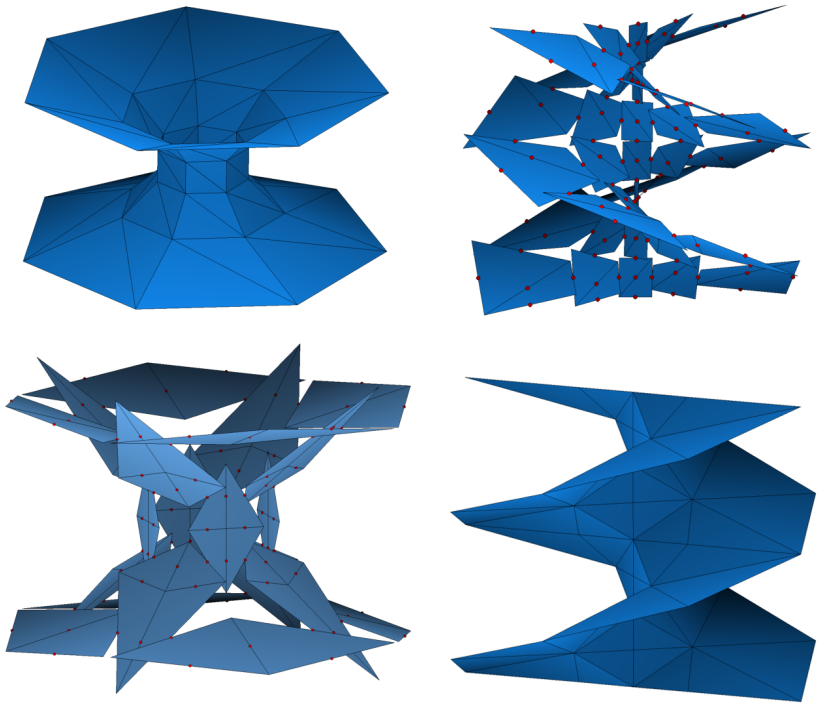

Fig. 4 Conjugate pairs of a discrete catenoid and a helicoid in each row.

1.3 Discrete Conjugate Minimal Surfaces

We extend the notion of piecewise linear functions to vector-valued piecewise linear functions, i.e. simplicial maps $F : M_h \to \mathbb{R}^3$ denoted by $F \in S_h(M_h)^3$ resp. for edge-based representations denoted by $F^* \in S_h^*(M_h)^3$. The discrete Laplace-Beltrami operator $\Delta_h F$ is defined by applying 6 to the component functions of F. In the special case of $F = id_{M_h}$ its Laplace becomes the *discrete mean curvature vector* of M_h with versions at vertices

$$H(p) := \Delta_h id_{M_h}(p) \in T_p\mathbb{R}^3$$

and at edges

$$H(m) := \Delta_h^* id_{M_h}^*(m) \in T_m\mathbb{R}^3$$

which measures the variation of discrete surface area in the space of conforming $F(M_h)$ or non-conforming meshes $F^*(M_h)$.

Surfaces with mean curvature $H = 0$ are called *discrete minimal surfaces* since they are critical points of the discrete area functional. From $H = 0$ follows that the component functions of the identity map id_{M_h} are discrete harmonic, thus have conjugate harmonic pairs. Therefore, the conjugacy of harmonic maps extends to the conjugacy of discrete minimal surfaces composed of a pair of a conforming and a non-conforming discrete minimal surface. See Figure 4 with a pair of a conforming catenoid and a non-conforming helicoid, resp. its reverse representations in the second row. See Figure 14 with several more discrete minimal surfaces with a smooth quad-parametrization.

1.4 Discrete Hodge-Helmholtz Decomposition

The Hodge-Helmholtz decomposition of vector fields on surfaces provides a precise criterion for the local integrability properties of vector fields as well as their relation to globally defined harmonic vector fields. Later we will make flexible use of all three Hodge components of vector fields. As an example see Figure 5 where a vector field on a simplicial torus is decomposed.

Theorem 3 (Hodge-Helmholtz decomposition). *The space of piecewise constant vector fields $\Lambda^1(M_h)$ on a simplicial surface M_h decomposes into an L^2-orthogonal sum of the spaces of gradient fields, co-gradient fields and harmonic fields:*

$$\Lambda^1 = \nabla S_h \oplus \delta S_h^* \oplus (H := \operatorname{curl}_h^* \cap \ker \operatorname{div}_h)$$

$$v = \underbrace{\nabla f}_{\operatorname{curl}_h^* \nabla f = 0} \oplus \underbrace{\delta g}_{\operatorname{div}_h \delta g = 0} \oplus \underbrace{w}_{\operatorname{curl}_h^* w = \operatorname{div}_h w = 0}$$

This space of discrete harmonic fields H on a compact 2-surface of genus g has correct dimension $2g$. The roles of the conforming S_h and non-conforming S_h^* spaces may be exchanged.[13].

Proof. The gradient and co-gradient part of v can be computed by minimizing a quadratic energy, the harmonic part is then obtained as remainder. The gradient component of $v \in \Lambda^1$ is the unique minimizer of

$$\min_{f \in S_h} \int_{M_h} \|v - \nabla f\|^2$$

and the co-gradient component is the unique minimizer of

$$\min_{g \in S_h^*} \int_{M_h} \|v - \delta g\|^2$$

w.r.t. to appropriate boundary conditions. It is easy to show that curl and div components of the minimizer vanish.

Remark 2. Depending on applications, both spaces might be chosen of the same type when the correct dimension of H is negligible.

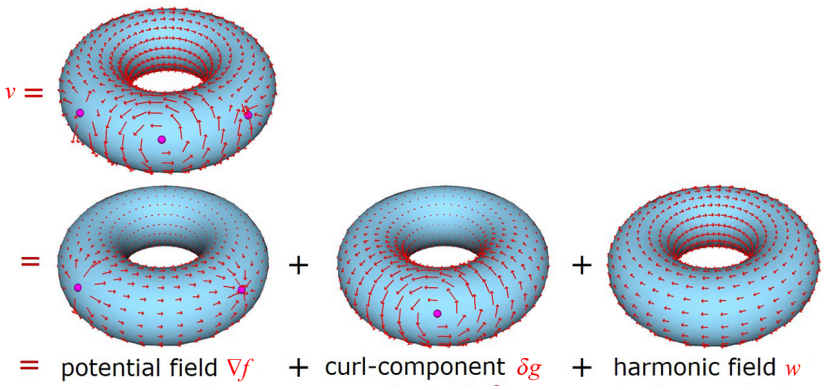

Fig. 5 Hodge decomposition of a piecewise constant tangent vector field on a simplicial torus to a gradient, co-gradient and harmonic field.

2 Mesh Parametrization

Triangle meshes are among the popular data structures for surface representations in computer graphics, geometry processing and finite element numerics.

They provide a rich flexibility, for example, for adaptive mesh refinement according to local resolution needs, and they come along with a large set of efficient processing algorithms. On the other hand, sometimes more restrictive representations such as quad meshes are preferable. For example, when trying to convert a mesh into a hierarchical subdivision surface, or when panelizing a roof construction in architecture with simple planar glass panels, or when trying to compute a morph between two scans of a pair of characters in computer animations.

Assume two characters have been scanned and each scan is given as a high-precision mesh with millions of triangles, see Figure 6. A morphing between the two scans requires a bijective map between the two triangles meshes, certainly with additional restrictions of low distortion etc. Computing a homotopy automatically is typically very difficult and no perfect algorithm exists yet. In practice, computer animators generate a matching to a large extent by hand: on both meshes the same quad layout is drawn, thus generating a bijective correspondence between points and quads of the two meshes, which then extends to a smooth morphing of the two shapes. Here an automatic mapping algorithm would be more than appreciated and is currently the target of intensive research activities in geometry processing.

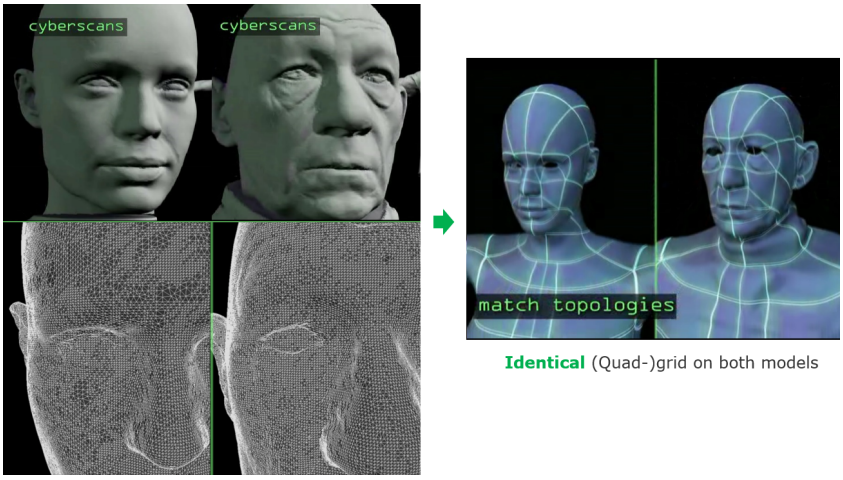

Fig. 6 Morphing a pair of 3d scans of two characters is currently performed by constructing two matching grids on both models by hand (images by Beau Janzen).

2.1 QuadCover Parameterization

We now use the discrete concepts derive in the previous sections to formulate the basic principles of the QuadCover algorithm [5] as an example and application of discrete differential geometric concepts to the solution of the intriguing problem of surface parametrization in geometry processing.

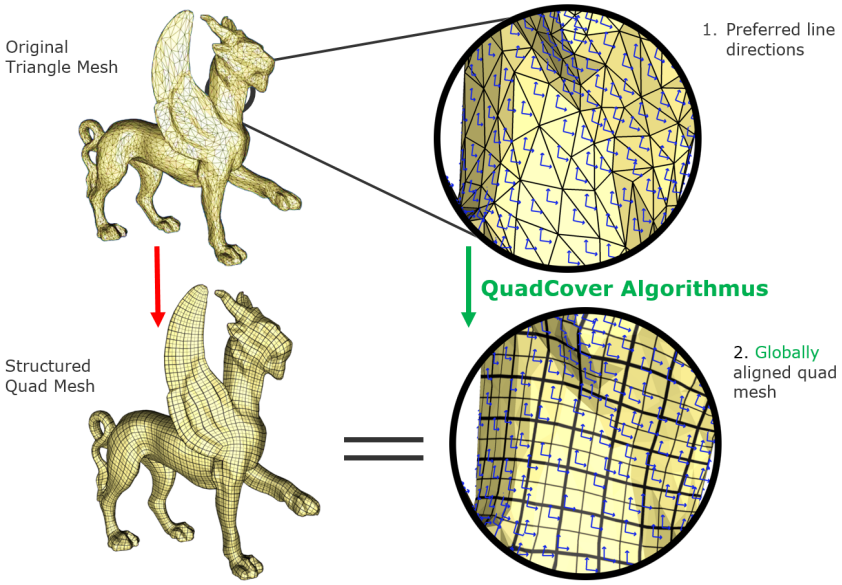

Fig. 7 QuadCover algorithm for quad-meshing guided by a frame field is described exactly in discrete differential geometry concepts.

The QuadCover algorithm takes as input a triangle mesh plus a guiding frame field X on M_h, see Figure 7. Formally, a *frame field* X on M_h consists of a pair of constant vectors $X_T = (X_1, X_2)_T$ in each triangle $T \in T_{M_h}$. In our application, it is convenient to extend a frame field X to a *cross field* $(X_1, X_2, -X_1, -X_2)$, also denoted by X. The continuity of a cross field across the common edge $e_{ij} = T_i \cap T_j$ of two adjacent triangles T_i and T_j is given by a periodic jump $r_{ij} \in \{0, 1, 2, 3\}$ denoting the pairing of the first vector X_1 on T_i with the $r_{ij} - th$ vector in the adjacent triangle T_j; for simplicity we assume orthogonal frames in this description. Overall this edge pairing produces a well-defined continuous frame field resp. cross field on M_h, see Figure 8.

The two tangent vectors of a frame field are intended to direct the parameter lines, namely, that optimally the parameter lines at each point are tangent to the two guiding vectors. The two additional directions of a cross

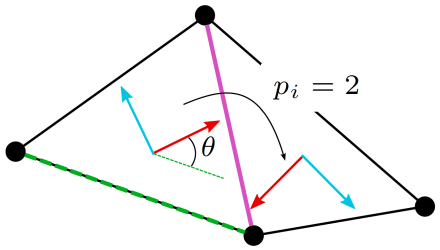

Fig. 8 Encoding the continuity of a frame field across the common edge of two adjacent triangle.

field guide the same parameter lines, just in opposite direction. A frame field may be obtained either automatically as principal curvature directions of a discrete shape operator or a field may be carefully design to follow surface features or even aesthetic reasoning.

A central statement is, given a triangle mesh plus a frame field, then the QuadCover algorithm provides a merely exact and reliable computational algorithm for the generation of an *atlas of charts* which generates a globally consistent quad-layout on the surface. The inverse φ^{-1} of each chart φ maps the Z^2-grid of $\mathbb{R}^2$ onto the surface such that parameter lines are optimally aligned in direction of the guiding frame field, see Figure 9. More precisely, a chart $\varphi \in S_h \times S_h : M_h \to \mathbb{R}^2$ is a simplicial map from the surface M_h to the texture domain $\mathbb{R}^2$. Using φ^{-1} the $\mathbb{Z}^2$-grid of the texture domain is mapped as texture onto the surface, such that the $\mathbb{Z}^2$-lines are tangential to the guiding frame field. An atlas of charts $\{\varphi_i\}$ is computed such that their inverses φ_i^{-1} generate a consistent quadrilateral grid $\left\{\varphi_i^{-1}\left(\Omega_i \cap \mathbb{Z}^2\right)\right\}$ on M_h. Note, that grid on M_h is given as texture map, that means at this stage as a functional representation on M_h.

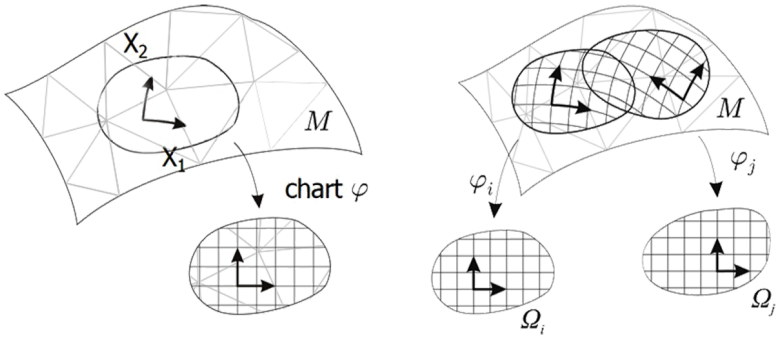

Fig. 9 A chart on a simplicial surface (left) with fulfilled compatibility condition for quad-parametrization (right).

From a computer graphics point of view, the charts are nothing else than element based texture maps from the surface M_h to the Euclidean texture domain $\mathbb{R}^2$. That means that the images of triangles may not be connected to the images of adjacent triangles and there corresponds on chart φ_i to each triangle T_i. The *compatibility of condition* on the charts of a quad-based parametrization requires that the images of two triangles $\{T_i, T_j\} \subset M_h$ with non-empty common edge $e_{ij} = T_i \cap T_i$ are mapped to two triangles $\varphi_i(T_i)$ and $\varphi_j(T_j)$ such that the common edge is mapped to two edges $\varphi_i(e_{ij})$ and $\varphi_j(e_{ij})$ which are translated by an integer vector or rotated by a multiple of $90°$ or a combination of both. This compatibility condition on the atlas assures continuity of the grid lines on M_h, see Figure 12.

QuadCover Algorithm

The main steps of the QuadCover algorithm are given below, relying on the discrete concepts introduced in the previous sections. For technical reasons we use a cross field instead of a frame field. Assume a simplicial surface M_h with cross field X is given. Then:

1. (Lift to 4-fold covering space) We lift the cross field to a 4-fold branched covering surface M_h^* of the mesh M_h, where each triangle is covered by four triangles of M_h^*. The four vectors of the cross field on M_h can be lifted to a single PC vector field X^* on M_h^* where each of the four vectors of the cross is lifted to a specific layer of M_h^*, such that maximal continuity is assured.
2. (Local integrability via Hodge) Compute the locally non-integrable curl-component $\delta g \in \delta S_h^*(M_h^*)$ of the vector field X^* on M_h^* and remove it $\overline{X^*} := X^* - \delta g$. Locally, $\overline{X^*}$ is now integrable and has a potential function.
3. (Global integrability via harmonic fields) The global matching of the grid spacing along all loops (so-called *global integrability*) requires that the path integrals of $\overline{X^*}$ along all homology loops $\gamma \in H_1(M_h^*)$ are integer valued. This integrability property is obtained by a correction of $\overline{X^*}$ by the L^2-smallest harmonic field $w \in H$ such that

$$\int_\gamma \overline{X^*} + w \in \mathbb{Z} \text{ for all homology loops } \gamma.$$

   Since the dimension of the space discrete harmonic fields is equal to the dimension of the first homology group $H_1(M_h^*)$, the minimizers exists. Note, harmonic fields are curl*-free, therefore the corrected field $\widetilde{X^*} := \overline{X^*} + w$ is still locally integrable.
4. (Integration) The vector field $\widetilde{X^*}$ is by 2. locally and by 3. globally integrable, thus on each chart on M_h^* we can solve the 1^{st}-order PDE $\widetilde{X^*} = \nabla\varphi^*$ with a function $\varphi^* \in S_h(M_h^*)$. On each chart, φ^* projects to four functions $(\varphi_1, \varphi_2, -\varphi_1, -\varphi_2)$ with $\varphi_i \in S_h(M_h)$ giving the compo-

nent functions of the simplicial chart $\varphi = (\varphi_1, \varphi_2) : M_h \to \mathbb{R}^2$, the texture map we were looking for.

Note, step 1 is necessary since frame fields and cross fields typically do not globally decompose into vector fields, thus the Hodge theorem would not apply without the introduced 4-fold covering. Practically, the 4-fold covering surface is usually never created and all information stored otherwise.

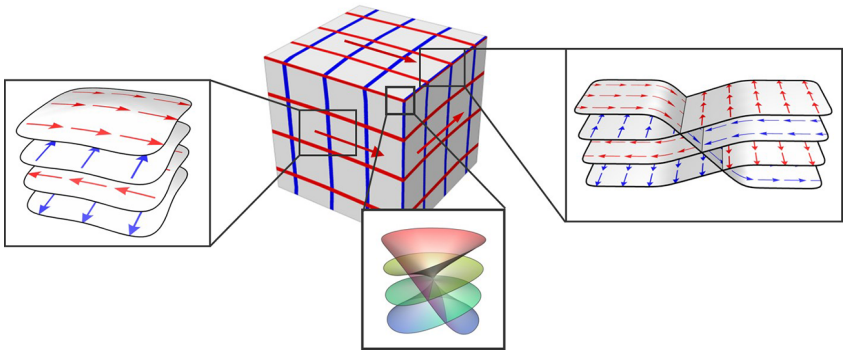

Fig. 10 Lifting a frame field to a vector field on a 4-fold branched simplicial covering surface .

The level lines of the chart functions φ^* on M_h^* obtained in the above process will project to the parameter lines on M_h we are looking for. Equivalently, the level lines of the two component functions of the projected chart function $\varphi = (\varphi_1, \varphi_2)$ on M_h directly yield the pair of parameter lines on M_h.

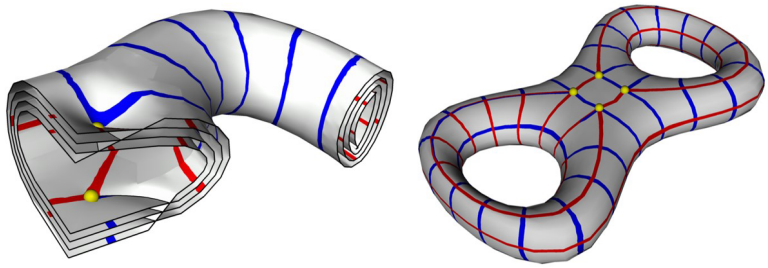

Fig. 11 The level lines of the generated potential function on M_h^* compose to the quad nets on M_h after projection.

Some sample applications are shown on the two figure tables 14 and 15.

2.2 Implementation Issues

Smooth frame fields are often generated from principal curvature directions, if the surface is smooth. The shape operator on simplicial surfaces derived in [4] provides a reliable pair of principal curvature directions. Due to the instability of umbilical regions for principal curvature computations, often curvature directions are generated in a sparse set of trusted regions and then extended using parallel transport to unreliable regions to cover the whole surface. These extensions are smoothed either by a direct rounding approach [5], an iterative rounding approach [2] or using holomorphic energies [7]. Typically, orthogonal frame fields are used, but non-orthogonal frame fields are possible too, for recent work see also [11].

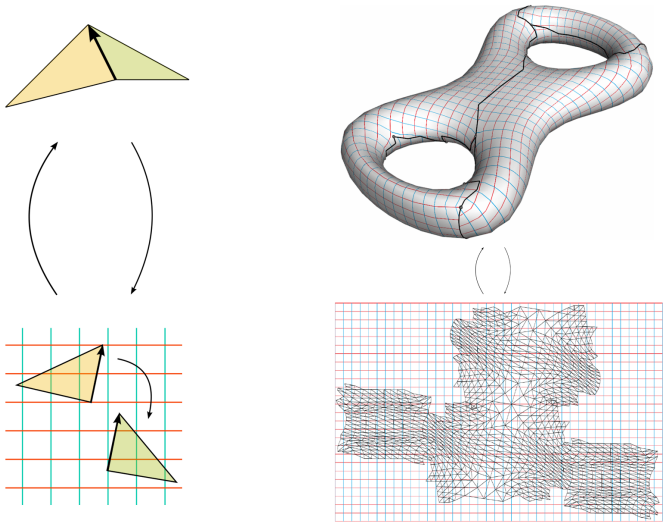

Fig. 12 Transition function between a pair of triangle based charts (left) and an atlas on a simplicial pretzel realized by a set of triangle based charts (right).

The principal idea behind the optimization is to find a texture map whose per triangle gradients align best to the input frame fields. The Hodge energy is either linearized by taking partial derivatives or put into a quadratic form. Solving the two linear systems is fast and widely used in frame field-driven parameterization methods [5],[2],[8],[3]. Unfortunately, it does not guarantee injectivity so that recent methods [1] rather minimize the quadratic energy using advanced non-linear solvers. The size of the system, in both methods, can be dramatically reduced by first introducing a dual spanning tree which defines a cut graph and then observing that the transition functions between triangle charts must be a grid automorphism [5] in $\mathbb{R}^2$. The cut graph is nec-

essary to be able to flatten the mesh in a 2D domain. The grid automorphism condition assures the local integrability of the resulting parameterization.

Notice that the parameterization generated by the least square minimization has seams along the cut path of the geometry. This is due to the local integrability of the curl free frame field. To obtain a globally continuous parameterization, the translation vector $\mathbf{t}_{ij}$ must be an integer translation, i.e. $\mathbf{t}_{ij} \in \mathbb{Z}^2$ and the singularities must be mapped to integer points or a mixed of grid mid points and integer points. Adding these constraints to the list square minimization makes the problem a mixed integer optimization which is an NP-hard problem. Several heuristics have been proposed to approximate the solution. The QuadCover algorithm [5] uses a simultaneous rounding via corrections with harmonic vector fields along the homology generators. The Mixed Integer Quadrangulation [2] approaches the problem by an iterative rounding which approximate a better solution at the cost of a slower running time. Recent methods consider the problem as a mixed integer quadratic problem [1] which aims at the global minimum of the energy. Figure 13 shows some examples of seamless parameterization using different rounding strategies.

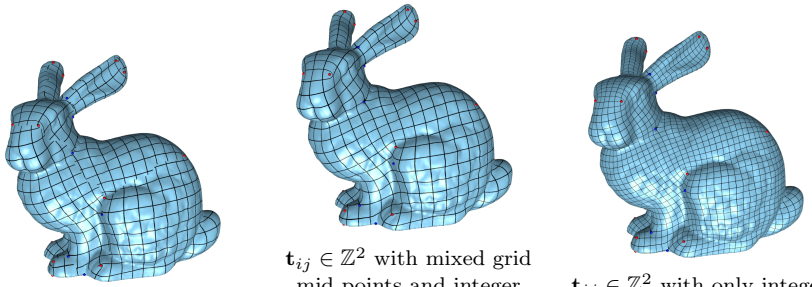

Fig. 13 Generation of seamless parameterizations using different rounding strategies generated by QuadCover.

The QuadCover algorithm is implemented based on JavaView available at `www.javaview.de`.

2.3 Examples of Parameterizations

We give some example of parameterizations generated by the QuadCover algorithm, among them are minimal and constant mean curvature surfaces as

well as non-orientable surfaces such as the Klein bottle. A second slide shows the generalizations StripeCover [6] and HexCover [9] for stripe covering and hex-covering. The CubeCover algorithm [10] is an extension to 3d volumetric meshes which converts a tetrahedral mesh with 3D frame field to a uniform cubical mesh aligned with the surface boundary.

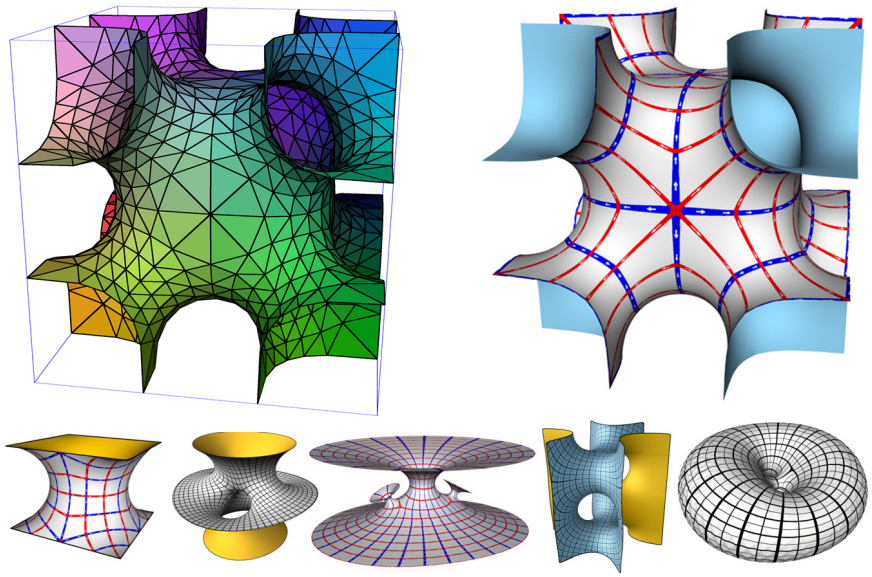

Fig. 14 QuadCover parametrizations of discrete minimal and constant mean curvature surfaces with boundary alignment.

References

1. D. Bommes, M. Campen, H.-C. Ebke, P. Alliez, and L. Kobbelt. Integer-grid maps for reliable quad meshing. *ACM Trans. Graph.*, 32(4):98:1–98:12, July 2013.
2. D. Bommes, H. Zimmer, and L. Kobbelt. Mixed-integer quadrangulation. *ACM Trans. Graph.*, 28(3):77:1–77:10, July 2009.
3. M. Campen and L. Kobbelt. Quad layout embedding via aligned parameterization. *Computer Graphics Forum*, 33:69–81, 2014.
4. K. Hildebrandt and K. Polthier. Generalized shape operators on polyhedral surfaces. *Computer Aided Geometric Design*, 28(5):321 – 343, 2011.
5. F. Kälberer, M. Nieser, and K. Polthier. Quadcover - surface parameterization using branched coverings. *Comput. Graph. Forum*, 26(3):375–384, 2007.
6. F. Kälberer, M. Nieser, and K. Polthier. Stripe parameterization of tubular surfaces. In V. Pascucci, H. Hagen, J. Tierny, and X. Tricoche, editors, *Topological Methods in Data Analysis and Visualization. Theory, Algorithms, and Applications.*, Mathematics and Visualization. Springer Verlag, 2010.

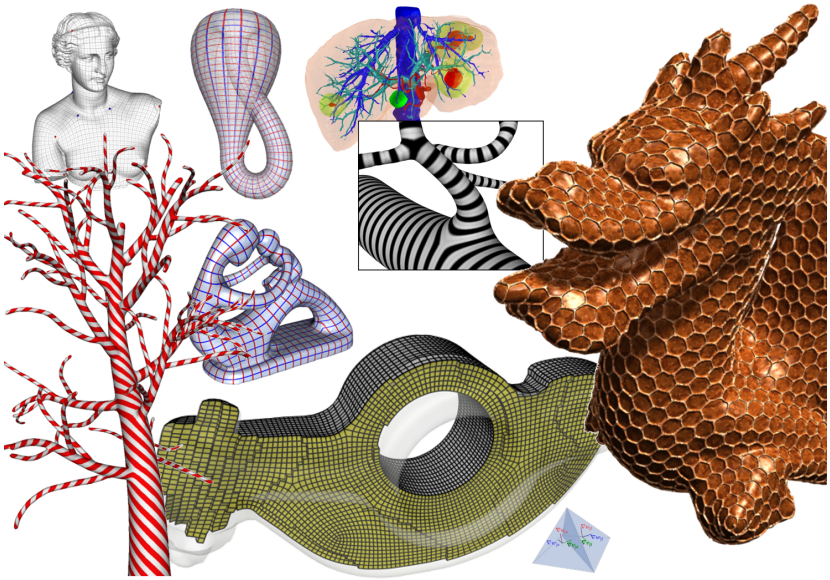

Fig. 15 Extensions of QuadCover to stripe and hexagonal parametrizations, as well as its generalization to CubeCover, the cubification of 3d volumes.

7. F. Knöppel, K. Crane, U. Pinkall, and P. Schröder. Globally optimal direction fields. *ACM Trans. Graph.*, 32(4), 2013.
8. A. Myles, N. Pietroni, D. Kovacs, and D. Zorin. Feature-aligned t-meshes. *ACM Trans. Graph.*, 29(4):1–11, 2010.
9. M. Nieser, J. Palacios, K. Polthier, and E. Zhang. Hexagonal global parameterization of arbitrary surfaces. *IEEE Transactions on Visualization and Computer Graphics*, 18(6):865–878, 2012.
10. M. Nieser, U. Reitebuch, and K. Polthier. CubeCover - parameterization of 3d volumes. *Computer Graphics Forum*, 30(5):1397–1406, 2011.
11. D. Panozzo, E. Puppo, M. Tarini, and O. Sorkine-Hornung. Frame fields: Anisotropic and non-orthogonal cross fields. *ACM Trans. Graph.*, 33(4):134:1–134:11, July 2014.
12. K. Polthier. Unstable periodic discrete minimal surfaces. In S. Hildebrandt and H. Karcher, editors, *Geometric Analysis and Nonlinear Partial Differential Equations*, pages 127–143. Springer Verlag, 2002.
13. K. Polthier and E. Preuss. Identifying vector field singularities using a discrete Hodge decomposition. In H.-C. Hege and K. Polthier, editors, *Visualization and Mathematics III*, pages 113–134. Springer Verlag, 2003.